Kinetics of Catalytic Cracking Selectivity in Fixed, Moving, and Fluid Bed Reactors

VERN W. WEEKMAN, JR., and DONALD M. NACE

Mobil Research and Development Corporation, Paulsboro, New Jersey

A kinetic mathematical model of catalytic cracking is described which accounts for conversion and gasoline yield in isothermal fixed, moving, and fluid bed reactors. The model has been tested and verified by using laboratory moving bed data with a commercial gas oil and catalyst. It is shown that under certain conditions, the selectivity behavior and maximum gasoline yield of fixed, fluid, and moving bed reactors will be identical. Maximum gasoline yield is defined in terms of both the kinetic parameters and the process variables for fixed, moving, and fluid bed reactors.

The catalytic cracking of a petroleum gas oil results in a broad spectrum of a products ranging from hydrogen and methane to heavy polymeric material adhering to the catalyst as coke. This range of products is normally separated into marketable fractions such as liquid petroleum gas, gasoline, light fuel oil, etc. Most attempts to describe the reaction kinetic behavior of catalytic cracking have been limited to the conversion behavior. Conversion is typically defined as that fraction of the original charge oil which has been converted to the gasoline boiling range and lighter. The work of Blanding (*2*), of Andrews (*1*), and of Weekman (*16*) are examples of the kinetics of catalytic cracking conversion.

Theoretical treatments of the effect of various types of catalyst decay on the selectivity of fixed bed reactions have been made by Froment and Bischoff (*6*), and by Masamune and Smith (*8*). Sagara, Masamune, and Smith (*13*) have treated catalyst decay in terms of time dependent effectiveness factors for isothermal and nonisothermal cases. Carberry and Gorring (*3*) have shown the consequences of progressive pore mouth poisoning, and Olson (*10*) has extended this work and showed the effects of an adsorbing guard chamber. Sada and Wen (*12*) have analyzed the effects of pore mouth poisoning on selectivity behavior, and Chu (*4*) has included a Langmuir-Hinshelwood kinetic model to study adsorptive catalyst fouling. Ozawa and Bischoff (*11*) employed a linear decay law based on carbon formed in describing the kinetics of *n*-hexadecane cracking on silica-alumina catalyst. Recently, Szepe and Levenspiel (*14*) in a general study of catalyst deactivation have shown that a simple m^{th} order decay law is adequate to describe many cases of catalyst fouling.

In earlier work (*16*), it was shown that conversion kinetics, when coupled with catalyst decay, adequately describe a wide range of conversion behavior. In the present paper, the kinetic description will be extended to include gasoline production and the subsequent recracking of gasoline. The gasoline selectivity model has been generalized to include the instantaneous behavior of fixed bed reactors as well as the steady state behavior of moving, fluid, or riser type of reactors.

THE SELECTIVITY MODEL

In the present treatment, we will reduce the broad spectrum of catalytic cracking charge stocks and products into a three-component system, namely, the original charge material, the gasoline boiling fraction (C_5^- 410°F.), and finally the remaining C_4's (dry gas and coke). This vastly simplified system can be justified on the basis that it enables us to understand the interaction between the process variables and the kinetic parameters of reaction velocity and catalyst decay velocity. On a purely economic basis, the gasoline fraction represents the most significant contribution to the overall profitability of the catalytic cracking reactor. This simplified reaction system is shown below as Equation (1):

$$C_1 \xrightarrow{k_0} a_1 C_2 + a_2 C_3 \qquad (1a)$$

$$C_2 \xrightarrow{k_2} C_3 \qquad (1b)$$

Here, C_1 represents the gas oil charged, while C_2 represents the C_5-410°F. gasoline fraction and C_3 the butanes, dry gas, and coke. The a_1 and a_2 coefficients represent the mass of C_2 produced per mass of C_1 converted, respectively. Whether the molecule of C_1 is split instantaneously to form both C_2 and C_3, or whether it reacts in parallel to form C_2 and C_3, is immaterial from a modeling point of view, since identical equations results for either reaction scheme. For an isothermal, vapor-phase, plug flow reactor with negligible interparticle diffusion, it is possible to describe the reactions shown in Equations (1) in terms of two coupled continuity equations given below:

$$\frac{\partial y_1}{\partial t} + U_v \frac{\partial y_1}{\partial z} = -R_1(y_1, t) \qquad (2a)$$

$$\frac{\partial y_2}{\partial t} + U_v \frac{\partial y_2}{\partial z} = a_1 R_1(y_1, t) - R_2(y_2, t) \qquad (2a)$$

The time dependent rate of reaction terms for gas oil and gasoline cracking are shown as $R_1(y_1, t)$ and $R_2(y_2, t)$, respectively.

The rate terms R_1 and R_2 represent the instantaneous rate of reaction in a differential element of the reacting space. The catalyst contributes to the reaction velocity; however, the catalyst activity declines as the reaction proceeds. Thus the reaction rate will also be a function of the catalyst residence time in the reactor.

The apparent cause of the decline of the catalyst activity is the adsorption of polynuclear aromatic compounds which polymerize to form a coke deposit typical of spent catalytic cracking catalysts. For a wide variety of typical catalytic cracking feedstocks, the catalytic carbon produced as a consequence of the cracking reactions is the most significant cause of catalyst decay. It was first shown by Voorhies (*15*) that the rate of carbon formation is largely a function of the catalyst residence

time and essentially independent of the rate of oil throughput. Thus it is possible to represent the catalyst decay as only a function of the catalyst residence time. This decay refers only to the temporary loss in catalyst activity and not to the long-term catalyst decay which occurs with repeated regenerations.

For heavier gas oil feeds with significant Conradson carbon content, a so-called *additive coke* also is formed, and its rate of deposition is determined mostly by the oil throughput rate. This type of aging is not considered in the present paper.

It has been shown previously that the kinetics of gas oil cracking can reasonably be represented as a second-order reaction coupled with catalyst decay (*16*). These kinetics are given below:

$$R_1 (y_1, t) = k_0 \Phi_1 (t) y_1^2 \tag{3}$$

The second-order kinetics are shown later in the report to represent experimental data quite well. Pure hydrocarbons are known to crack according to a first-order rate law [Crocoll and Jaquay (5) and Nace (9)]; however, the second-order law reflects the fact that the constituents of gas oil exhibit a wide spectrum of cracking rates. Thus, as we crack deeper into the gas oil, the cracking rate increasingly slows down, and the overall effect is well approximated by a second-order reaction. Blanding (2) arrives at a similar conclusion but employs a different argument.

The gasoline, representing a narrower boiling fraction, will exhibit a smaller range of cracking rates. Because of this fact, a first-order reaction is assumed for gasoline cracking. This relation is shown below:

$$R_2 (y_2, t) = k_2 \Phi_2 (t) y_2 \tag{4}$$

Equations (2) may be simplified if we normalize them by employing a dimensionless distance $x = z/z_0$ and a dimensionless time $\theta = t/t_c$. The vapor velocity U_v is given as follows:

$$U_v = \frac{F_0}{\rho_v \Omega} \tag{5}$$

The normalized forms of Equations (2) in terms of the liquid hourly space velocity (based on the liquid charge density and the reactor volume) are:

$$S = \frac{F_0}{\rho_l V_r} \tag{6}$$

$$B \frac{\partial y_1}{\partial \theta} + \frac{\partial y_1}{\partial x} = - \frac{\rho_0}{\rho_l S} k_0 \Phi_1 y_1^2 \tag{7a}$$

$$B \frac{\partial y_2}{\partial \theta} + \frac{\partial y_2}{\partial x} = \frac{\rho_0}{\rho_l S} [k_1 \Phi_1 y_1^2 - k_2 \Phi_2 y_2] \tag{7b}$$

where

$$B = \frac{\rho_v V_r}{F_0 t_c} = \frac{t_v}{t_c}$$

$$k_1 = a_1 k_0$$

As shown previously (*16*), B represents the characteristic of Equations (7) and is the ratio of vapor to catalyst residence time. The ρ_v term on the right-hand side has been replaced with ρ_0 (vapor density if no reaction), since the variation in vapor density can be adsorbed in the second-order reaction approximation. For steady state reactors such as moving and fluid beds, the time derivatives of Equations (7) are exactly zero. For fixed beds, the vapor transit time is usually much less than the catalyst residence time, and therefore $B \cong 0$. In other words, if individual oil molecules traverse the length of the reactor so fast relative to the catalyst decay that they see catalyst of essentially uniform age, we may drop the time derivatives even for fixed beds. Equations (7) may now be reduced to the following simplified ordinary differential equation form:

$$\frac{dy_1}{dx} = - \frac{K_0}{S} \Phi_1 y_1^2 \tag{8a}$$

$$\frac{dy_2}{dx} = \frac{K_1}{S} \Phi_1 y_1^2 - \frac{K_2}{S} \Phi_2 y_2 \tag{8b}$$

where

$$K_i = \frac{\rho_0 k_i}{\rho_l}$$

These equations apply to any plug flow, isothermal reactor, be it fixed, fluid, or moving bed. However, to solve Equations (8), we must specify the nature of the catalyst decay function which in turn depends on the catalyst residence time. Two different functions which have been found to adequately represent experimental cracking data are given as follows:

$$\Phi_i = e^{-\alpha_i t_c} \quad \text{(first-order decay)} \tag{9}$$

$$\Phi_i = 1/t_c^{n_i} \quad (t_c^n \text{ decay}) \tag{10}$$

The catalyst-to-oil ratio may be introduced by noting that for any reactor, the catalyst/oil ratio is a function of the catalyst residence time and the space velocity [$\beta = 1/(t_c S)$].

Since it appears reasonable that the same type of catalyst sites which crack gas oil molecules will also crack gasoline range molecules, we can make the simplifying assumption that $\Phi_1 = \Phi_2$. It is now possible to define a stretched or distorted reaction time u by the following transformation:

$$du = \frac{\Phi}{S} dx \tag{11}$$

Equations (8) may now be reduced to the following elementary forms:

$$\frac{dy_1}{du} = - K_0 y_1^2 \tag{12a}$$

$$\frac{dy_2}{du} = K_1 y_1^2 - K_2 y_2 \tag{12b}$$

The stretched time u will be a function of the nature of catalyst decay function Φ and the catalyst residence time t_c. In Table 1, the forms of u for commonly employed cracking reactors are listed in terms of a dimensionless extent of reaction group $A = K_0/S$ for both first-order and t_c^n type of decay.

The fluid bed reactor forms in Table 1 result from the assumption of perfectly mixed catalyst flow with plug gas flow. This model is, of course, an oversimplification, since the presence of gas bubbles leads to a dilute-dense phase model which is widely discussed in the literature. However, the simplified model is useful in comparing the gross behavior of fixed, fluidized, and moving bed reactors. An average reaction velocity constant for this case may be defined as

$$\overline{k} = k_0 \int_0^\infty I(\theta) \Phi(\theta) d\theta \tag{13}$$

The internal age distribution $I(\theta)$ for a perfectly mixed vessel is $e^{-\theta}$, and thus for first-order and t_c^n decay the average reaction velocities are, respectively

$$\overline{k} = k_0 \int_0^\infty e^{-\theta} \cdot e^{-\lambda\theta} d\theta = \frac{k_0}{1 + \lambda} \tag{14}$$

$$\overline{k} = k_0 \int_0^\infty e^{-\theta} (t_c \theta)^{-n} d\theta = \frac{k_0 \Gamma(1 - n)}{t_c^n} \tag{15}$$

where $\Gamma(1 - n)$ is the incomplete gamma function of

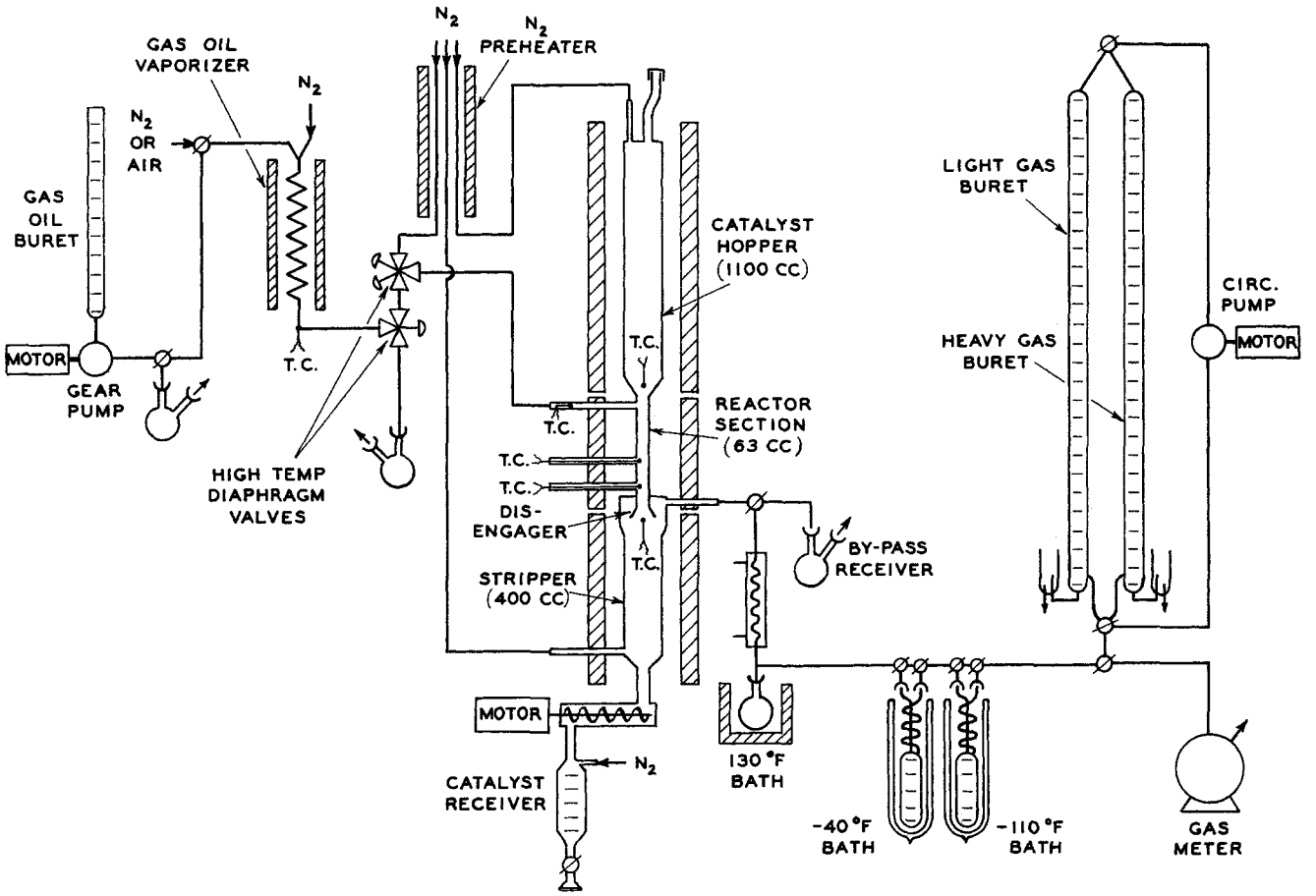

Fig. 1. Schematic drawing of the moving bed cracking unit.

$1 - n$.

SOLUTIONS FOR CONVERSION BEHAVIOR

Fortunately, Equation (12*a*) may be solved in closed form for various reactor geometries and first-order decay in terms of an extent of reaction group $A_0 = K_0/S$ and an extent of decay group $\lambda = \alpha t_c = \alpha/\beta S$. These solutions are detailed elsewhere (*16*) and are listed in Table 2 for convenience. Also listed in Table 2 are the conversion solutions for the t_c^n type of model. In general, the first-order model yields more convenient mathematical forms, although both decay functions yield solutions of Equations (12) which are quite similar for typical cracking parameters.

The time averaged solutions are listed, since much catalyst screening work takes place in fixed bed reactors in which the products are allowed to accumulate over the course of reaction. As shown in the previous work cited, the first-order decay solutions matched very well with fixed bed experimental data from zeolite catalysts. In an earlier paper, the selectivity behavior of fixed beds was treated in more detail (*17*).

SOLUTIONS FOR SELECTIVITY BEHAVIOR

Simultaneous solution of Equations (12) to yield both conversion $(1 - y_1)$ or gasoline yield (y_2) is not possible in terms of simple functions. A solution in terms of the tabulated exponential integral function is possible which is much more efficient than solving the equations numerically. By dividing Equation (12*b*) by Equation (12*a*), the following relationship results:

$$\frac{dy_2}{dy_1} = \left(\frac{K_2}{K_0}\right)\frac{y_2}{y_1^2} - \frac{K_1}{K_0} \tag{16}$$

Solution of this equation with the boundary condition of no initial gasoline (that is, $y_1 = 1$, $y_2 = 0$) yields the desired solution in terms of the selectivity ratios $r_1 = K_1/K_0$ and $r_2 = K_2/K_0$:

$$y_2 = r_1 r_2 e^{-r_2/y_1}\left[\frac{1}{r_2}e^{r_2} - \frac{y_1}{r_1}e^{r_2/y_1} - Ein(r_2) + Ein\left(\frac{r_2}{y_1}\right)\right] \tag{17}$$

where $Ein(x) = \int_{-\infty}^{x} \frac{e^x}{x}\,dx$.

It is thus possible to combine the solutions for conversion $(1 - y_1)$ listed in Table 2 with Equation (17) to represent the effect of the process variables on the conversion and gasoline yields.

EXPERIMENTAL

In order to obtain steady state catalytic cracking data, a bench-scale unit having a moving catalyst bed reactor was built. A schematic drawing of this unit is shown in Figure 1. The reactor utilizes concurrent flow of oil and 14/20 mesh catalyst in a ½-in. diameter isothermal reactor. Hot catalyst moves from a 1-liter hopper through the 63-cc. volume reaction section and then through a stripping zone where residence time is six times longer than in the reactor. A screw conveyer below the stripping section removes catalyst from the system and thus moves the catalyst through the reactor at a rate depending on the speed of the motor driving it. Plug flow of catalyst in the reactor section was demonstrated in a duplicate glass model of the apparatus.

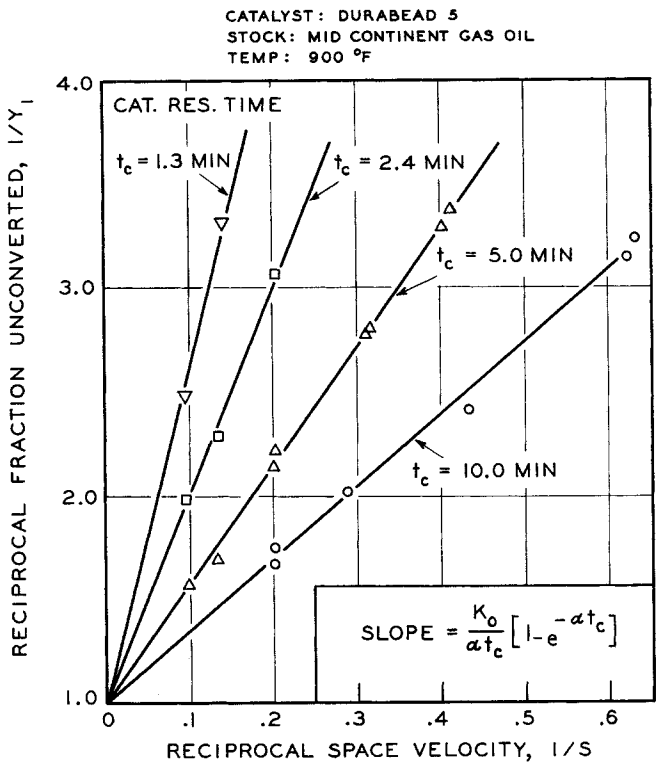

Fig. 2. Second-order test of moving bed data.

Gas oil, which has been completely vaporized by pumping through a 900°F. preheater, is charged to the top of the reactor section. Nitrogen corresponding to 14% of vaporized gas oil is added in the preheater. The gas oil preheater is connected to the reactor through two high temperature, stainless steel, diaphragm valves. These valves are used to bypass the vaporized gas oil stream around the reactor until a steady state is reached at the desired vapor temperature, at which time it is then directed into the downflow reactor. A nitrogen purge through the catalyst hopper further dilutes the entering gas oil vapors to a partial pressure of 0.78 atm. for all runs.

The range of catalyst flow rates allows catalyst residence time to be varied from 1 to 10 min. in the reactor. Generally 70 to 180 cc. of gas oil were charged, and from 400 to 600 cc. of

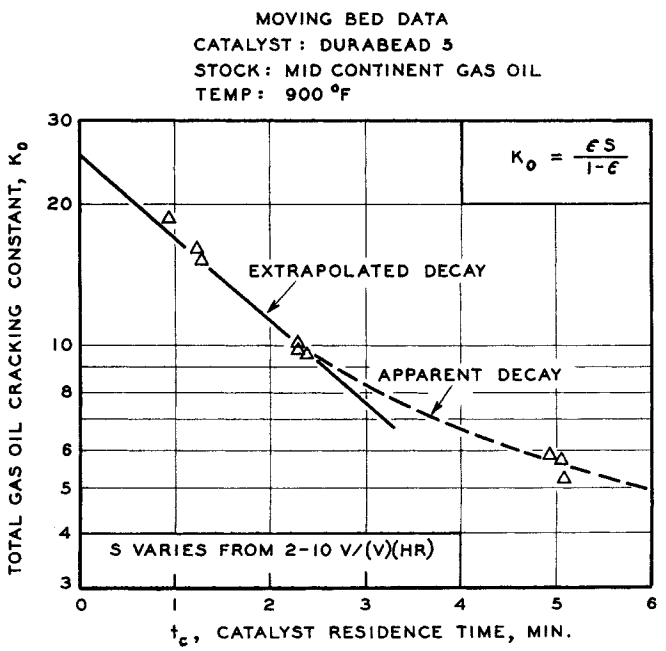

Fig. 3. Extrapolation for initial catalyst activity.

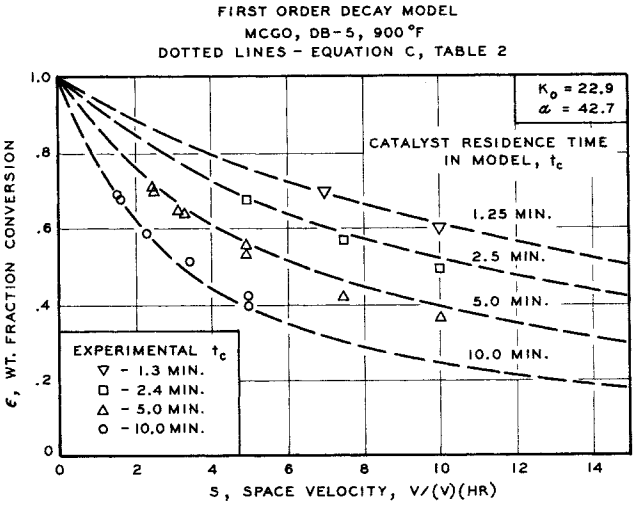

Fig. 4. Comparison of model with moving bed conversion data.

catalyst were passed through the reactor during a balance run. Prior to making a balance run, however, a prerun was made for a period of time equal to three times the catalyst residence time in the reactor to ensure steady state reaction conditions for the subsequent balance run period. Products were bypassed from the product collection system during the prerun through a valve on the reactor outlet line.

Product analyses involved collecting and sampling a light gas which had passed through traps at −40° and −110°F. and a heavy gas produced by weathering all condensed liquid products at 135°F. The weathered liquid products were distilled to a 410°F. vapor temperature gasoline end point.

The gas oil used in the experiments is a wide range 29.6°API gravity Mid-Continent blend with a boiling range of 423° to 904°F. The catalyst is a zeolite containing commercial TCC catalyst ground to 14/20 mesh particle size.

COMPARISON OF MODEL WITH EXPERIMENTAL CONVERSION AND SELECTIVITY DATA

The model requires the determination of four constants: the reaction velocity constant, the gas oil cracking rate constant, the gasoline formation rate constant, and the gasoline cracking rate constant. In general, these constants were obtained by a nonlinear parameter estimation method due to Marquardt (7); however, as will be shown below, some graphical procedures also work well.

To test the second-order nature of the gas oil cracking reaction, we can rewrite Equation (c) in Table 2 as follows:

$$\frac{1}{y_1} = 1 + \frac{1}{S}\left[\frac{K_0}{\alpha t_c}\left(1 - e^{-\alpha t_c}\right)\right] \qquad (18)$$

Thus, if we hold the catalyst residence time t_c constant, the term in brackets is constant, and a plot of $1/y_1$ vs. $1/S$ should yield a straight line with origin at 1.0 and slope

Table 1. Stretched Reaction Times u

	First-order catalyst decay	t_c^n catalyst decay
Fixed beds	$\frac{xe^{-\lambda\theta}}{S}$	$\frac{x}{St_c^n}$
Moving beds (plug catalyst flow)	$-\frac{e^{-\lambda x}}{\lambda S}$	$\frac{x^{1-n}}{(1-n)\,St_c^n}$
Fluid beds (perfect mixed catalyst flow)	$\frac{x}{(1+\lambda)S}$	$\frac{x\Gamma(1-n)}{St_c^n}$

TABLE 2. SOLUTIONS OF EQUATION (12a) FOR CONVERSION ϵ

First-order decay
$A_0 = K_0/S \quad \lambda = \alpha t_c = \alpha/\beta S$

Fixed bed

$$\epsilon = \frac{A_0 e^{-\lambda}}{1 + Ae^{-\lambda}} \text{ (instantaneous)} \qquad (a)$$

$$\bar{\epsilon} = \frac{1}{\lambda} \text{Ln} \left[\frac{1 + A_0}{1 + A_0 e^{-\lambda}} \right] \text{ (time averaged)} \qquad (b)$$

Moving bed

$$\epsilon = \frac{A_0 (1 - e^{-\lambda})}{\lambda + A_0 (1 - e^{-\lambda})} \qquad (c)$$

Fluid bed*

$$\epsilon = \frac{A_0}{1 + \lambda + A_0} \qquad (d)$$

t_c^n decay
$A_0 = K_0/S \quad \gamma = (\beta S)^n = t_c{}^{-n}$

Fixed bed

$$\epsilon = \frac{A_0 \gamma}{1 + A_0 \gamma} \text{ (instantaneous)} \qquad (e)$$

$$\bar{\epsilon} = \int_0^1 \frac{A_0 \gamma}{\theta^n + A_0 \gamma} d\theta \text{ (time averaged)} \qquad (f)$$

Moving bed

$$\epsilon = \frac{A_0 \gamma}{1 - n + A_0 \gamma} \qquad (g)$$

Fluid bed*

$$\epsilon = \frac{A_0 \gamma \Gamma(1 - n)}{1 + A_0 \gamma \Gamma(1 - n)} \qquad (h)$$

* Perfectly mixed solid phase, plug flow gas phase.

$(K_0/\alpha t_c)(1 - e^{-\alpha t_c})$.

From Figure 2 we see that the experimental moving bed data do indeed plot as a second-order reaction over a wide range of conditions. Furthermore, for the longest catalyst residence time of 10 min., the exponential term in Equation (6) will be negligible, and K_0/α may be calculated directly from the slope as 0.575.

As the catalyst residence time approaches zero, it can be shown that the limit of Equation (9) is

$$\lim_{t_c \to 0} y_1 = \frac{1}{1 + K_0/S} \qquad (19)$$

Thus, for very short catalyst residence times in a moving bed, we can solve directly for K_0 from Equation (7):

$$K_0 = \frac{1 - y_1}{y_1} S \qquad (20)$$

However, since experimental data can only be obtained at finite catalyst residence times, we must extrapolate to zero time. Figure 3 shows such an extrapolation for the shortest time data giving an intercept of 25. From Figure 2 it was determined that $K_0/\alpha = 0.575$ and, therefore, $\alpha = 42.5$. To test the data at intermediate catalyst residence times, it is necessary to resort to nonlinear regression on Equation (18). This regression yielded $K_0 = 22.9$ and $\alpha = 42.7$ which compare most favorably with the estimates obtained graphically from both long and short catalyst residence times.

From Figure 4 we see that the moving bed model, with these two constants used, fits the experimental data well with a standard deviation of ±2.2% conversion.

By combining Equation (17) and Equation (c) in Table 2 with Marquardt's nonlinear estimation method, it was possible to evaluate the two remaining constants, K_1 and K_2, from the experimental data. These constants were determined as $K_1 = 18.1$ and $K_2 = 1.7$. The ratio of K_1 and K_0 (that is, a_1) shows that the initial gasoline formation efficiency of this catalyst-charge-stock combination is 0.79. By using all four constants in Equation (17) and Equation (c) of Table 1, it was possible to develop the curves shown in Figure 5. When compared with the experimental gasoline data, we see that the mathematical model represents the actual behavior quite well. The model's prediction of zero gasoline yield at zero space velocity results, of course, from the assumed reaction sequence and reaction order. The match of the mathe-

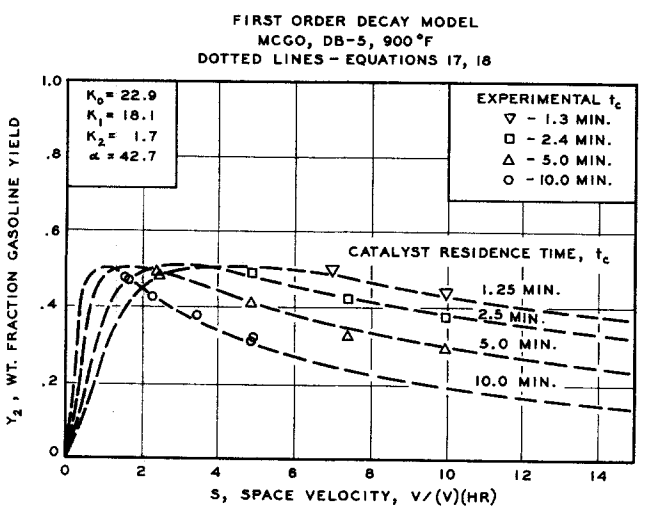

Fig. 5. Comparison of gasoline yield with experimental moving bed data.

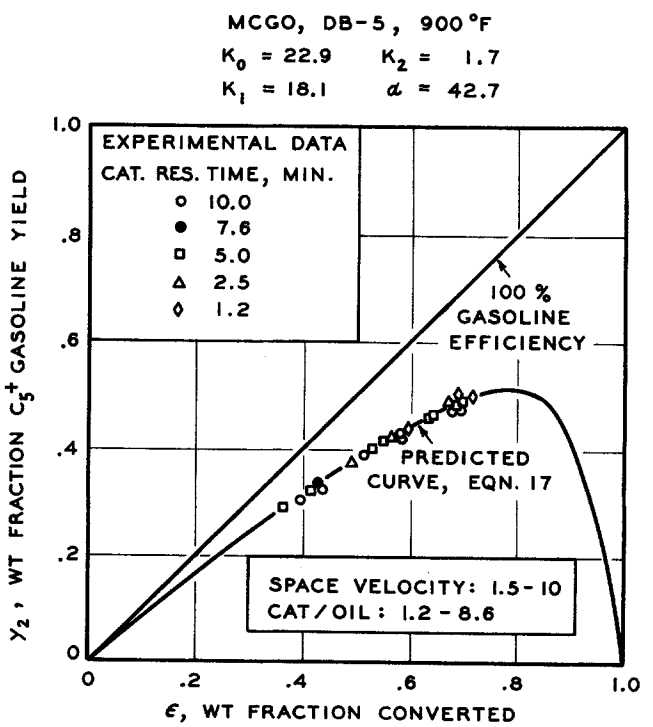

Fig. 6. Comparison of model with moving bed data.

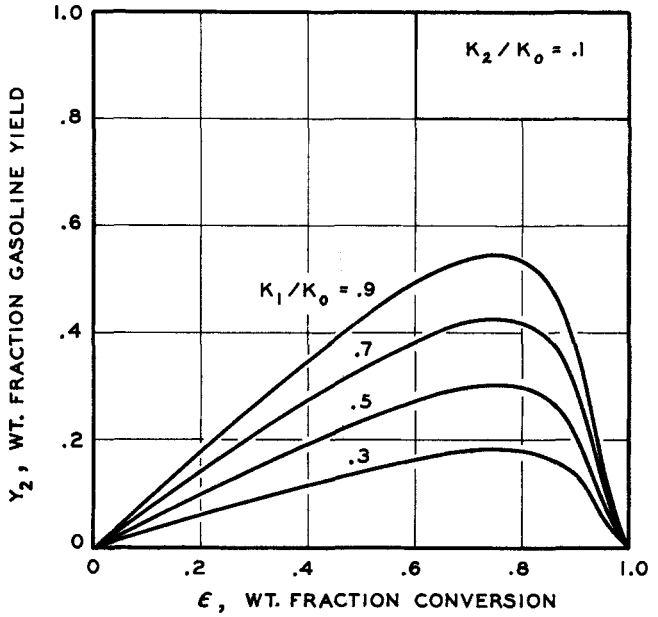

Fig. 7. Effect on selectivity of varying initial selectivity ratio at constant gasoline-to-gas oil cracking ratio.

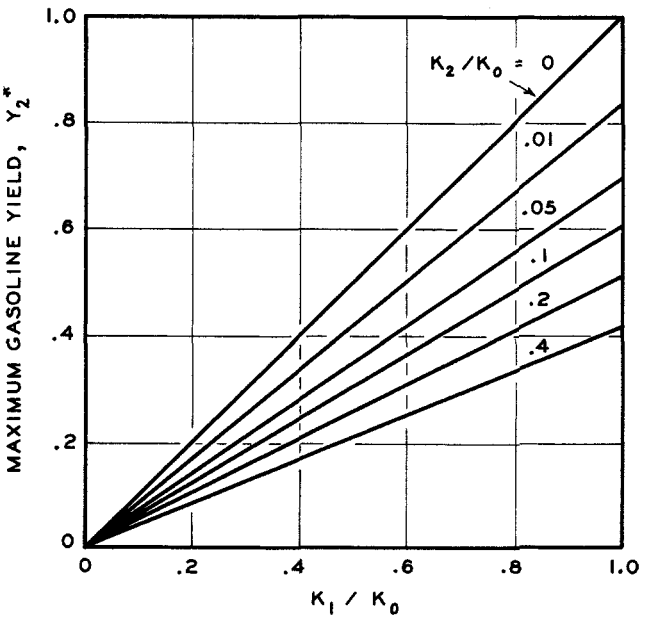

Fig. 9. Maximum instantaneous gasoline yield (equal decay of all catalyst functions).

matical model to experimental data shows a standard deviation of only ±1.5 wt. % gasoline.

By using the same parameter estimation method, it was possible to obtain the n and K_0 constants required by the t_c^n model given as Equation (g) in Table 2. The decay constant n was found to be 0.72, and the cracking rate constant K_0 was shown to be 0.266 for the gas oil used. A combination of Equation (17) with Equation (g) in Table 1 permitted the remaining constants of K_1 and K_2 to be determined for the t_c^n model. These constants were 0.214 and 0.0188, respectively. A comparison of the t_c^n model with the experimental conversion and gasoline yield revealed that the fit was even slightly better than the first-order model. The curves for the t_c^n model were almost identical with those of the first-order model shown on Figures 4 and 5. As shown by Equation (17), the selectivity behavior depends solely on the ratio of the rate constants, and thus the absolute value of the rate constants for either decay model are quite different owing to the nature of the decay function. The ratios of the rate constants are quite similar as shown in Table 3.

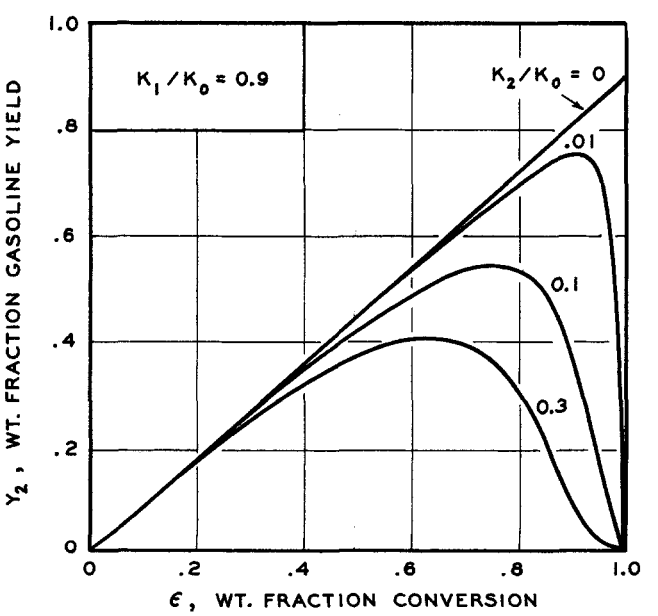

Fig. 8. Effect on selectivity of varying gasoline-to-gas oil cracking ratio at constant initial selectivity.

SELECTIVITY BEHAVIOR

A plot of conversion vs. gasoline yield is commonly used as the main guide in evaluating catalyst performance. This type of selectivity plot can be readily generated by Equation (17).

It is most important to note that Equation (17) is independent of space velocity, catalyst residence time, catalyst/oil ratio, and even the form of the decay function. Indeed it depends only on the initial selectivity ratio (K_1/K_0) and the overcracking ratio (K_2/K_0). Since K_0, K_1, and K_2 are functions only of temperature, such a selectivity plot will exhibit no parametric effect of any other process variable. If Equation (17) is valid, the strong parametric effect of space velocity and catalyst residence time observed for conversion and gasoline yield separately should disappear on a conversion vs. gasoline plot. Figure 6 compares a plot of Equation (17), with the previously determined constants with the experimental data. Thus, for a tenfold range of space velocity and catalyst residence time, Equation (17) describes the experimental results quite well. The parametric effect of space velocity and catalyst residence time largely disappear on the selectivity plot as predicted by the simple theory.

Since Equation (17) is independent of catalyst residence time, it holds for moving beds (or riser crackers) and fluid beds as well as for the instantaneous selectivity of fixed bed reactors (that is, prior to any time averaging). The maximum gasoline yield, as shown on Figure 6, will thus be the same for any vapor-phase, plug flow, reactor system if the gas oil and gasoline cracking activities decay at the same rate.

While the set of experimental data shown on Figure 8 did not achieve a high enough conversion to show the

Table 3. Rate Constant Ratios

	K_1/K_0	K_2/K_0
First-order decay model	0.79	0.074
t_c^n decay model	0.80	0.071

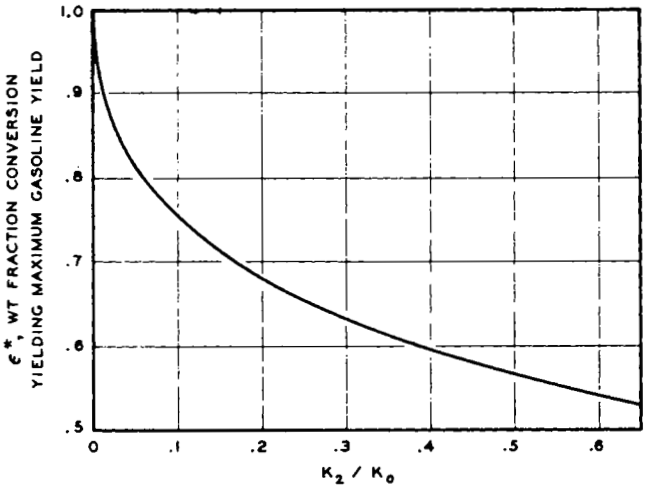

Fig. 10. Conversion yielding maximum gasoline yield as a function of gasoline-to-gas oil cracking ratio.

maximum in the selectivity behavior, the effect is commonly seen in cracking data at high conversions. In an earlier paper (*17*), data are presented for conversions well beyond the maximum selectivity point. It would be hazardous to extrapolate to high conversions if only very low conversion data were available, since the accuracy of determining the gasoline cracking constant K_2 improves with increasing conversion.

The effect of the rate constant ratios K_1/K_0 and K_2/K_0 on the general selectivity behavior are shown as Figures 7 and 8. From Figure 7 we see the effect of the initial selectivity ratio K_1/K_0 as the gas oil-to-gasoline cracking ratio is held constant. The initial slope of the selectivity plot is exactly K_1/K_0. On Figure 8 the overcracking ratio K_2/K_0 is varied, while K_1/K_0 is held constant. In general, K_2/K_0 has the greatest effect at high conversion levels, while the initial selectivity ratio changes the selectivity curve the most at low conversions.

MAXIMUM GASOLINE YIELD

Since gasoline production plays such a large economic role in catalytic cracking, we will explore the properties of the maximum possible gasoline yield in more detail. Since the maximum gasoline yield will occur when dy_2/dy_1 is equal to zero, we can employ Equation (16) to give us the necessary conditions for a maximum yield. This relationship is shown as Equation (21):

$$y_2^\circ = \frac{K_1}{K_2}(1-\epsilon^\circ)^2 \qquad (21)$$

Table 4. Process Variable Conditions for Maximum Gasoline Yield

Fixed Bed

$$S^\circ = \frac{K_0\, e^{-\alpha t_c}}{\left[\sqrt{\frac{K_1}{K_2\, y_2^\circ}} - 1\right]}$$

Moving bed

$$S^\circ = \frac{K_0\,(1-e^{-\alpha t_c})}{\alpha t_c\left[\sqrt{\frac{K_1}{K_2\, y_2^\circ}} - 1\right]}$$

Fluid bed

$$S^\circ = \frac{K_0}{(1+\alpha t_c)\left[\sqrt{\frac{K_0}{K_2\, y_2^\circ}} - 1\right]}$$

Table 5. Activations in Calories Per Gram Mole, Mid-Continent Gas Oil, Commercial Zeolite Catalyst

Q_0	Q_2	Decay
10,000	18,000	−1,700

By combining Equations (17) and (21), it is possible to solve for the maximum gasoline yield in terms of the initial selectivity ratio K_1/K_0 and the gasoline cracking ratio K_2/K_0. The results of these calculations are shown as Figure 9, and they allow one to readily estimate the maximum gasoline yield from the two selectivity ratios. From Figure 7, it can be seen that the conversion level which yields the maximum gasoline yield is independent of the initial selectivity ratio K_1/K_0. This can be proved by substituting Equation (21) into Equation (17) and by noting that the K_1/K_0 ratio cancels out. Thus, the conversion level which gives the maximum gasoline yield depends only on the gasoline cracking ratio K_2/K_0. Figure 10 presents the conversion which yields the maximum gasoline yield as a function of the gasoline-gas oil cracking rate K_2/K_0.

The maximum gasoline yield can also be related to the normal process variables by combining Equation (21) with the conversion relationships given in Table 2. The results of these substitutions for the first-order decay model are given in Table 4. These equations give the space velocity required to achieve the maximum gasoline yield for any value of the catalyst residence time. The required maximum gasoline yield y_2° can be read directly from Figure 8. These same equations can also be used to compute the catalyst residence time required for the maximum gasoline yield at any given space velocity. Such relationships will be useful for designing a reactor system to produce maximum gasoline yield for a given catalyst and charge stock. For existing units, the relationships can be used to assign the space velocity and catalyst residence time which will give a maximum in gasoline production.

EFFECT OF TEMPERATURE ON SELECTIVITY

Activation energies for the gas oil cracking reaction Q_0 and the gasoline cracking reaction Q_2 were determined

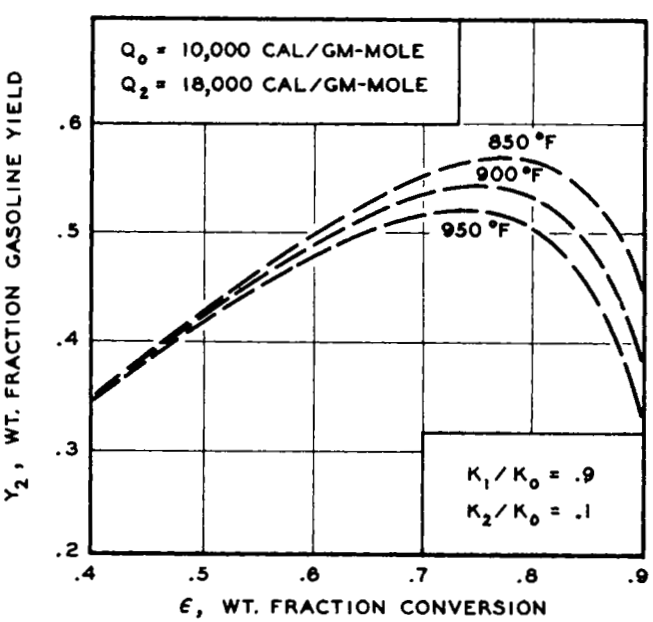

Fig. 11. Effect of temperature on gasoline selectivity.

with the laboratory moving bed equipment at 900° and 970°F. It was also observed that the decay velocity constant α decreased with increasing temperature. One possible explanation is that decreased adsorption of heavy aromatic molecules more than compensates for the increase in catalytic coke as temperature is raised. The reaction activation energies and the decay activation are given in Table 5.

It should be noted that the gasoline cracking activation energy is almost twice that of the gas oil cracking. Thus, as temperature is lowered, the gasoline cracking rate declines more than the gas oil cracking rate, and a higher selectivity results. Figure 11 shows an example of this behavior as derived from Equation (17) for various temperatures.

An interesting optimal problem is posed by this difference in activation energies. From Figure 11, we see that lower temperatures yield a higher maximum selectivity, but from Table 4 we note that for all reactors, if catalyst residence time is held constant, we must go to a lower space velocity to achieve the conversion which yields the maximum gasoline yield. Clearly we face an optimum temperature problem; as we lower temperature, we trade increased reactor cost and decreasing octane number against increased selectivity. For an existing reactor, we trade throughput and octane number against increased selectivity.

SUMMARY

A kinetic mathematical model has been developed for catalytic cracking which accounts for conversion and gasoline production in isothermal fixed, moving, and fluid bed reactors. The model has been tested and verified by using laboratory moving bed data with a commercial gas oil and catalyst. It has been shown that when both the gas oil and gasoline cracking functions of the catalyst decay at the same rate, the selectivity behavior of fixed, fluid, and moving bed reactors will be identical. A maximum gasoline yield exists and is the same for all three types of reactors. Maximum gasoline yield is defined in terms of both the kinetic parameters and the process variables for fixed, moving, and fluid bed reactors. Since the gas oil and the gasoline cracking rate have different activation energies, an optimum reactor temperature is indicated.

NOTATION

A_i = extent of reaction group for species i, ratio of reaction to space velocity, $\rho_0 k_i/\rho_l S_0 = K_i/S$
a_1 = K_1/K_0
B = t_v/t_c
$Ein(x)$ = exponential integral function, $\int_{-\infty}^{x} \frac{e^x}{x} dx$
F_0 = oil charge rate, lb./hr., mass flow rate
k_i = reaction velocity constant of i^{th} reaction at $\theta = 0$, hr.$^{-1}$ (includes initial feed concentration because of second-order reaction)
$\bar{k}_i$ = mean average reaction velocity constant of i^{th} reaction
K_0 = gas oil cracking rate
K_2 = gasoline cracking rate
K_1 = $a_1 K_0$
K_i = $\rho_0 k_i/\rho_l$
n = decay constant in t_c^n model
Q_i = activation energy of reaction i, cal./(g.)(mole)
r_1 = K_1/K_0
r_2 = K_2/K_0
S = liquid hourly space velocity, vol./(vol.)(hr.)
t = clock time, hr.
t_c = catalyst residence time (under oil exposure conditions), hr.
t_v = vapor-phase residence time, sec.
u = stretched time variable defined by Table 1
U_v = vapor velocity, ft./sec.
V_r = reactor volume, cu. ft.
x = normalized axial distance, z/z_0
y_2^* = maximum gasoline weight fraction
y_i = instantaneous weight fraction of component i
$\bar{y}_i$ = time averaged weight fraction of component i
z = axial distance in reactor, ft.
z_0 = total reactor length, ft.

Greek Letters

α = decay velocity constant, hr.$^{-1}$
β = catalyst-to-oil ratio, vol.cat./vol. total oil for fixed bed; (vol.cat./hr.)/(vol.oil/hr.) for moving and fluid beds
$\Gamma(1-n)$ = incomplete gamma function with argument $1-n$
ϵ = instantaneous weight fraction converted
$\bar{\epsilon}$ = time averaged weight fraction converted
θ = normalized time-on-stream, t/t_c
λ = extent of catalyst decay group, $\alpha/\beta S$ or αt_c
ρ_0 = initial charge density at reactor conditions, lb./cu.ft.
ρ_l = density of liquid charge at room temperature, lb./cu.ft.
ρ_v = vapor density at reactor conditions
Φ = catalyst decay function
$\Phi_2(t)$ = gasoline cracking decay function
Ω = reactor cross sectional area, sq. ft.

Superscript

* = maximum condition

LITERATURE CITED

1. Andrews, J. M., *Ind Eng. Chem.*, **51**, 507 (1959).
2. Blanding, F. H., *ibid.*, **45**, No. 6, 1186 (1953).
3. Carberry, J. J., and R. L. Gorring, *J. Catalysis*, **5**, 529 (1966).
4. Chu, C., *Ind. Eng. Chem. Fundamentals*, **7**, 509 (1968).
5. Crocoll, J. F., and R. D. Jaquay, *Petro./Chem. Engr.*, **C-24** (Nov., 1960).
6. Froment, G. F., and K. B. Bischoff, *Chem. Eng. Sci.*, **16**, 189 (1961). *Ibid.*, **17**, 105 (1962).
7. Marquardt, D. W., *J. Soc. Ind. Appl. Math.*, **11**, No. 2, 431 (June, 1963).
8. Masamune, Shinobu, and J. M. Smith, *AIChE J.*, **12**, 384 (1966).
9. Nace, D. M., *Ind. Eng. Chem. Prod. Res. Develop.*, **8**, 24 (1969).
10. Olson, J. H., *Ind. Eng. Chem. Fundamentals*, **7**, 185 (1968).
11. Ozawa, Y., and K. B. Bischoff, *Ind. Eng. Chem. Process Design Develop.*, **7**, 72 (1968).
12. Sada, E., and C. Y. Wen, paper presented at 59th Annual Meeting, Am. Inst. Chem. Engrs., Detroit, Mich. (1966).
13. Sagara, M., Sinobu Masamune, and J. M. Smith, *AIChE J.*, **13**, 1226 (1967).
14. Szepe, S., and O. Levenspiel, paper presented at European Federation of Chemical Engineers on Reaction Engineering, Brussels Meeting (Sept., 1968).
15. Voorhies, A., Jr., *Ind. Eng. Chem.*, **37**, No. 4, 318 (1945).
16. Weekman, V. W., Jr., *Ind. Eng. Chem. Process Design Develop.*, **7**, No. 1, 90 (1968).
17. *Ibid.*, **8**, No. 3, 385 (1969).

Manuscript received July 26, 1968; revision received October 18, 1968; paper accepted October 21, 1968. Paper presented at AIChE New Orleans meeting.